Distributed atomic polarizabilities from electron density.
1. Motivations and Theory

Anna Krawczuk-Pantula,[a] Daniel Pérez, [a] Katarzyna Stadnicka,[b] Piero Macchi [a,]*

a) Department of Chemistry and Biochemistry, University of Bern, Freiestrasse 3, 3012 Bern, Switzerland

b) Faculty of Chemistry, Jagiellonian University, Ingardena 3, 30-060 Krakow, Poland

piero.macchi@dcb.unibe.ch

Abstract

In this paper, the distributed atomic polarizabilities computed within the Quantum Theory of Atoms in Molecules are discussed. Methods are presented to calculate and visualize symmetric atomic polarizability tensors, with proved additivity to molecular polarizabilities. The analysis of QTAIM bond polarizabilities is also presented for some simple molecules and potential applications in material science are anticipated.

Introduction

The response of electron density to an electric field is fundamental to understand, among the others, the behavior of molecules in chemical reactions, the solvation properties, the recognition processes and spectroscopic properties. As a matter of facts, the (hyper)polarizabilities tensors determine the soft ("orbital controlled") assembly and reactivity of molecules, the intensities of Raman scattering and many other optical processes. For this reason, measuring or calculating the molecular (hyper)polarizabilities is of fundamental importance, especially when dealing with material science. If the material is a crystalline solid, the properties are regulated by the electric susceptibilities, which are related, for molecular based materials, to the molecular (hyper)polarizabilities tensors through lattice summation.

Quantum chemistry allows to calculate (hyper)polarizabilities of molecules and crystals, by derivation of the electronic energy *E* with respect to the electric field *F*. For example, the first order polarizability tensor is defined as

$$\alpha_{ij} = -\frac{\partial^2 E}{\partial F_i \partial F_j} \qquad (1)$$

where α_{ij} is a component of the tensor. Because the derivative of energy with respect to the field is the dipole moment, α_{ij} can be calculated as the derivative of the dipolar moment with respect to the field.

$$\alpha_{ij} = -\frac{\partial^2 E}{\partial F_i \partial F_j} = \frac{\partial \mu_j}{\partial F_i} \qquad (2)$$

By definition, the polarizability tensor is symmetric.

Similarly to the charge distribution, a chemist would prefer to analyze the atomic and bond polarizabilities of a system rather than the total molecular quantity. There are many reasons. First of all, atoms and (functional) groups of atoms represent the way in which molecular chemists normally "reduce" a molecule (or a molecular crystal) for engineering purposes, in "old times" called *retro-synthesis*. In fact, the source of a given property may be localized in a subpart of the molecule. Moreover, atomic parameterization is a prerequisite for semi-empirical (force field based) modeling, used to compute the interaction energies between molecular fragments in molecular mechanics or dynamics simulations. For this purpose, transportable atomic polarizabilities are extremely useful. In fact, there have been several proposals for the calculation of distributed atomic polarizabilities, i.e. to decompose the total molecular polarizability into atomic contributions. This could be obtained either partitioning the energy or the electron density distribution in $\mathbf{R}^3$ or in Hilbert space. At this point, it is important to stress that in general a decomposition scheme is not correct or incorrect,

rather it is more or less useful. Partitioning in direct space has several advantages, in particular because it would be based on observables.

Stone (1985) and Sueur & Stone (1993) have for example proposed an expansion of the molecular polarizability in atom centered terms using a distributed multipole approach. They analyzed several ways to partition the molecular polarizability and they concluded that a space partitioned atomic polarizability volumes would be more efficient. Bader *et al.* (1987), Laidig & Bader (1987), Bader (1989) and Bader *et al.* (1992) proposed a hard space partitioning of the molecular polarizabilities, based on QTAIM, which was later generalized by Keith (2007). In fact, QTAIM offers the best space partitioning for atoms and a relatively simple numerical calculation of the atomic polarizabilities.

Hättig *et al.* (1996) have first proposed the atomic partitioning of frequency dependent polarizabilities, based on QTAIM as well as on Stone's approaches. Their main purpose was evaluation of atom-atom dispersion coefficients for the evaluation of intermolecular interaction energies. Gough *et al.* (1996) have used QTAIM polarizabilities to compute intensities of Raman spectra. However the results of atomic partitioning are missing in that work.

In this paper, ideas proposed by Keith are used as basis for the calculations of distributed atomic polarizabilities, with a more generalized treatment of ring structures, an extension of the quantities derived from atomic polarizabilities (like the bond polarizabilities) and a tentative connection with the unperturbed ground state electron density distribution.

Motivations

The motivations of our work are multifaceted. We are interested in computing, visualizing and analyzing atomic polarizabilities of some typical functional groups, providing an advanced tool to "standard" QTAIM analysis, including the possibility to define the bond polarizability. We also want to extract atomic polarizabilities using fuzzy partitioning schemes, like Hirshfeld stockholder atoms, to evaluate the more reliable and useful method. Moreover, we are interested in relating the ground state unperturbed electron density with the distributed atomic polarizabilities, in the attempt to estimate semi-empirical atomic and molecular polarizabilities from experimentally observable electron density distributions.

In a long term view, we expect to use transferable or semi-empirical atomic polarizabilities to estimate molecular and crystal properties, especially optical properties, and we are interested in visualizing the polarizability densities, as a tool to analyze chemical reactivity.

In this initial paper, we report on QTAIM distributed polarizabilities as a complement of normal QTAIM analysis, providing visualization tools for the atomic polarizabilities. The paper is structured as it follows: first we discuss the theoretical background and the partitioning scheme adopted, then we illustrate examples on some popular molecules, we discuss the results in terms of chemical and finally we anticipate further work.

Partitioning schemes

Among the possible partitioning scheme, we have focused on the spatial partitioning of the electron density, in keeping with the Quantum Theory of Atoms in Molecules

(QTAIM) by Bader (1987, 1990). Other authors have previously worked on calculating atomic polarizabilities from QTAIM, for example Keith (2007).

QTAIM offers some advantages, in particular the *same* and *exact* hard partitioning of the electron density and the electronic energy in $\mathbf{R}^3$. In fact, the molecular dipole moment or the molecular energy can be exactly decomposed into atomic components $\boldsymbol{\mu}(\Omega)$ or E(Ω), where Ω is the atomic basin volume. The dipole moment can be further decomposed into the *atomic polarization* $\boldsymbol{\mu}_p(\Omega)$ and the *charge transfer* $\boldsymbol{\mu}_c(\Omega)$ vectors. $\boldsymbol{\mu}_p(\Omega)$ comes from the integration of the dipolar density function $\mathbf{r}\rho(\mathbf{r})$ inside the atomic basin Ω. On the other hand, $\mu_c(\Omega)$ includes the weighted translation charge, moved from the atom center to all the related bond critical points (BCP). The direction and magnitude of this dipole depend on the nature and number of bonded groups to the selected atom.

$$\boldsymbol{\mu}(\Omega) = -\int_{\Omega} [\boldsymbol{r} - \boldsymbol{R}_0]\rho(\boldsymbol{r})d\boldsymbol{r} + \sum_{\Omega'} [\boldsymbol{R}_\Omega - \boldsymbol{R}_b(\Omega|\Omega')]Q(\Omega|\Omega') = \boldsymbol{\mu}_p(\Omega) + \boldsymbol{\mu}_c(\Omega) \tag{4}$$

where $Q(\Omega|\Omega')$ is the charge induced to atom Ω by the bond to atom Ω′, $\boldsymbol{R}_0$ is an arbitrary origin of coordinate system, $\boldsymbol{R}_\Omega$ is a positional vector of atom Ω and $\boldsymbol{R}_b(\Omega|\Omega'')$ is the positional vector of bond critical point between atom Ω and Ω'.

Noteworthy, this scheme overwhelms any origin dependence, of course in neutral molecules. To calculate the "charge transfer" contribution of a dipole moment the following conditions are imposed:

a) The sum of net atomic charges or sum of bond atomic charges is equal to the molecular charge:

$$Q^M = \sum_{\Omega=1}^{N_a} Q(\Omega) \tag{5}$$

where N_a is number of atoms and Q^M is the total molecular charge. In the simplest case, $Q^M = 0$.

b) Each atomic charge is the sum of all bond charges:[1]

$$Q(\Omega) = \sum_{\Omega' \neq \Omega}^{N_a} Q(\Omega|\Omega') \qquad (6)$$

where $Q(\Omega|\Omega') = 0$ if Ω and Ω' are not bonded. For each bond:

$$Q(\Omega|\Omega') + Q(\Omega'|\Omega) = 0 \qquad (7)$$

c) If a molecule contains a ring *R*, the sum of bond charges within the ring is equal to zero

$$\sum_{\Omega \in R} Q(\Omega|\Omega + 1) = 0 \qquad (8)$$

where Ω is an atom belonging to ring *R* and the summation requires that a given ring circulation is chosen (atom Ω is linked to Ω-1 and Ω+1; the first and last atoms in the sequence are also linked to each other).

Note, however, that equation (8) is only one of the main constraints that could be applied to a ring. In this simple formulation it corresponds to assume that all possible ring openings are equivalent, *i.e.* breaking the ring is identical at any bond. However, one could assign a weight to each bond, so that

$$\sum_{\Omega \in R} \lambda(\Omega|\Omega + 1) \cdot Q(\Omega|\Omega + 1) = 0 \qquad (9)$$

where $\lambda(\Omega|\Omega + 1)$ is a *bond weight*. In his formulation, Keith has basically assumed $\lambda(\Omega|\Omega + 1)$=1, whereas it should be more chemically reasonable to take these coefficients as inversely proportional to the bond strengths, for example measured by the electron density at the critical point between atoms Ω and Ω+1, $\rho(\Omega|\Omega + 1)$:

$$\lambda(\Omega|\Omega + 1) = \frac{1}{\rho(\Omega|\Omega+1)} \qquad (10)$$

[1] In case the total molecular charge is not zero, an additional constant should be added in equation (6), for example $\frac{Q^M}{N_a}$, in order to maintain the conditions (5) and (7).

This avoids that any sudden change of the molecular graph (like the formation of a weak bond nearby a catastrophe point in the configurational space) could create a huge discontinuity of the atomic moments hence of the polarizabilities, which is quite unrealistic. Thus, a weak bond would have a very small impact on bond charge partitioning within a ring. Obviously this is more important when the ring contains a weaker bond, such as a hydrogen bond or even weaker intermolecular contact.

Conditions (6) and (7) produce a system of equations that can be described in matrix notation:[2]

$$\mathbf{B}\mathbf{Q}_{\Omega|\Omega'} = \mathbf{Q}_{\Omega} \qquad (11)$$

where **B** is an atom-bond matrix (N_a x N_b), $\mathbf{Q}_{\Omega|\Omega'}$ is a vector (N_b) of the bond charges and $\mathbf{Q}_{\Omega}$ is the vector (N_a) of the atomic charges. The ring conditions are then used to build an extended **B'** matrix and a **Q'** ($\supset\mathbf{Q}_{\Omega}$) vector, so that the system of equations remains apparently over-determined and therefore soluble to obtain $\mathbf{Q}_{\Omega|\Omega'}$ after matrix inversion ($\mathbf{B'}^{-1}$).

As the dipole moment, the molecular polarizability can also be decomposed in additive atomic tensors:

$$\boldsymbol{\alpha} = \sum_{\Omega=1}^{N_a} \boldsymbol{\alpha}(\Omega) = \sum_{\Omega=1}^{N_a} [\boldsymbol{\alpha}_p(\Omega) + \boldsymbol{\alpha}_c(\Omega)] \qquad (12)$$

Where $\boldsymbol{\alpha}_p(\Omega)$ and $\boldsymbol{\alpha}_c(\Omega)$ are the atomic polarizability tensors coming from the derivation of the corresponding atomic dipoles with respect to the applied field.

This calculation can be carried out numerically, given the linear response of the electron density with respect to an applied field, at least for a small field. Thus,

$$\alpha_{ij}(\Omega) = \frac{\mu_i^{\varepsilon_j}(\Omega) - \mu_i^{0}(\Omega)}{\varepsilon_j} \qquad (13)$$

[2] Noteworthy, equation (5) just follows from (6) and (7).

where $\mu_i^{F_j}(\Omega)$ is the atomic dipolar component along the *i* direction computed with a given electric field (0 or ε) in direction *j*. In general, we have used calculation at $\pm \varepsilon_j$ and computed the derivatives by averaging the two dipole differences. Moreover, ε is a sufficiently small electric field (typically 0.005 a.u.) to guarantee a better extraction of the linear component of the electron polarization. For sake of simplicity, we do not take into account the coupling of atomic volume and atomic charge in evaluation of the dipole derivative. For this reason, the atomic polarizability tensors might result slightly asymmetric (depending on the point group symmetry of the atomic basin). This problem however, can be easily corrected through tensor symmetrization as recommended by Nye (1985). This is obtained from decomposing of the tensor $\boldsymbol{\alpha}$ into symmetric ($\boldsymbol{\alpha}^S$) and antisymmetric ($\boldsymbol{\alpha}^{AS}$) terms.

$$\boldsymbol{\alpha}^S = \frac{\boldsymbol{\alpha}+\boldsymbol{\alpha}^T}{2} \qquad (14)$$

$$\boldsymbol{\alpha}^{AS} = \frac{\boldsymbol{\alpha}-\boldsymbol{\alpha}^T}{2} \qquad (15)$$

As demonstrated in Table 1, this procedure reconstructs very accurately the total molecular polarizabilities (having the molecular polarizability from analytic energy derivatives as an exact benchmark). As a matter of facts, the antisymmetric components are basically cancelled each other when atomic components are summed up.

Noteworthy, all previous attempts to derive atomic polarizabilities from QTAIM partitioning reported only diagonal components of the atomic polarization tensors.

The symmetrized atomic polarizabilities are positive tensors and can be quite easily visualized in real space as ellipsoids, which axes have dimensions of volumes. Moreover, they can be easily exported from atoms calculated in simple molecules to atoms belonging to more complex systems (macromolecules or polymers, for

example). What is necessary is the definition of a proper local coordinate system that allows exporting the atomic parameters, see for example the discussion in Domagała, & Jelsch (2008). This is in keeping with what is generally proposed for transferable multipolar expanded atomic electron densities, based on experimentally determined parameters (Pichon-Pesme *et al.* (2004); Pichon-Pesme, Lecomte, & Lachekar (1995) Zarychta *et al.* (2007)) or theoretically calculated parameters (Volkov *et al.* (2004), Dittrich, B., Koritsanszky, T. & Luger, P. (2004); Dittrich *et al.* (2006) and Dominiak *et al.* (2007)). Thus, our proposal could simply complement the known transferability of multipolar electron density, including dipolar polarizability and it could be very easily implemented in the existing software. However, the transferable parameters should come from theoretical calculations.

Computational details

For a set of molecules analyzed in this paper, molecular wave functions were calculated at B3LYP/6-311++G(2p,2d) level, using Gaussian09. For di-carboxylic acids geometries were optimized and second derivatives of the energies were computed in order to calculate analytically the vibrational frequencies and the molecular polarizabilities. In case of aminoacids atomic coordinates were taken from neutron diffraction data and kept frozen for further calculations.

The static electron density distribution was also calculated with the same method at zero field as well as under small (0.005 a.u.) electric fields directed ($\pm$1,0,0), (0,$\pm$1,0) and (0,0,$\pm$1), respectively. This field was proven to be sufficiently small to obtain good numerical derivative of the dipolar density, but for glycine, where a field of 0.001 a.u. was necessary for a precise calculation.

It is interesting that the numerical derivative we applied (through 13) is also quite a rapid procedure to obtain molecular polarizabilities, because it requires only 7 single point calculations under electric field and relative integration of the electron density.

The QTAIM partitioning was applied using AIMAll software. Calculation of bond charges, atomic dipolar moments and dipolar polarizabilities was carried out with a locally developed routine (PolaBer) that will be described in details elsewhere. Visualization of the polarizability tensors was also carried out using a locally developed tool, which generates a X3D file representing the data as a 3D scene. The tensors are visualized in the same $\mathbf{R}^3$ space as the molecule, assuming that $1\text{Å}^3 \equiv 1\text{Å}$, though normally a scaling factor is necessary to reduce the size of polarizability ellipsoids for visualization purposes (the figures are produced with view3dscene, see Kamburelis (2011). In all pictures, we used a scale factor of 0.4Å^{-2} for the atomic polarizability tensors and 0.1Å^{-2} for the molecular polarizabilities.

Analysis of distributed atomic polarizabilities in test compounds

Using the theoretical background introduced above, we calculated QTAIM atomic polarizabilities for a number of organic molecules with potential interest also in material science, like amino acids, di-carboxylic acids etc. In fact, ammonium groups, carboxylates, olefins, etc. are typical functionalities of organic *linkers* employed in metal organic molecular materials, like for example metal organic frameworks. Moreover, amino acids are themselves receiving increasing attention as materials, in view of the intrinsic optical properties of their molecular crystals or co-crystals.

Table 1 Molecular polarizabilities calculated with QTAIM partitioning as described in the text (on the left) and calculated with analytical double derivation of Molecular energy respect to the field, as implemented in Gaussian09. All quantities are in atomic units (Bohr^3). The QTAIM molecular polarizabilities are obtained after tensor symmetrization.

	QTAIM partitioning (numerical calculation)	**Energy derivation (analytical calculation)**
Acetic acid	36.23 -0.79 0.00 -0.79 37.95 0.00 0.00 0.00 25.18	36.53 -0.75 0.00 -0.75 37.83 0.00 0.00 0.00 25.26
Oxalic acid	46.62 0.13 0.00 0.13 45.01 0.00 0.00 0.00 24.40	46.71 0.15 0.00 0.15 44.92 0.00 0.00 0.00 24.41
L-lactic acid	56.57 -0.49 0.53 -0.49 51.57 -2.75 0.53 -2.75 42.58	55.94 -0.44 0.52 -0.44 51.56 -2.75 0.52 -2.75 42.56
Glycine	48.22 -3.82 0.00 -3.82 63.27 0.00 0.00 0.00 33.20	48.16 -3.70 0.00 -3.70 61.92 0.00 0.00 0.00 33.19
L-alanine	71.25 4.83 0.56 4.83 61.20 -4.05 0.56 -4.05 49.27	70.44 4.68 0.48 4.68 61.09 -4.05 0.48 -4.05 49.18
L-tartaric acid	84.86 -0.10 -3.89 -0.10 72.01 -1.15 -3.89 -1.15 58.94	84.73 -0.21 -3.89 -0.21 72.07 -1.10 -3.89 -1.10 58.96

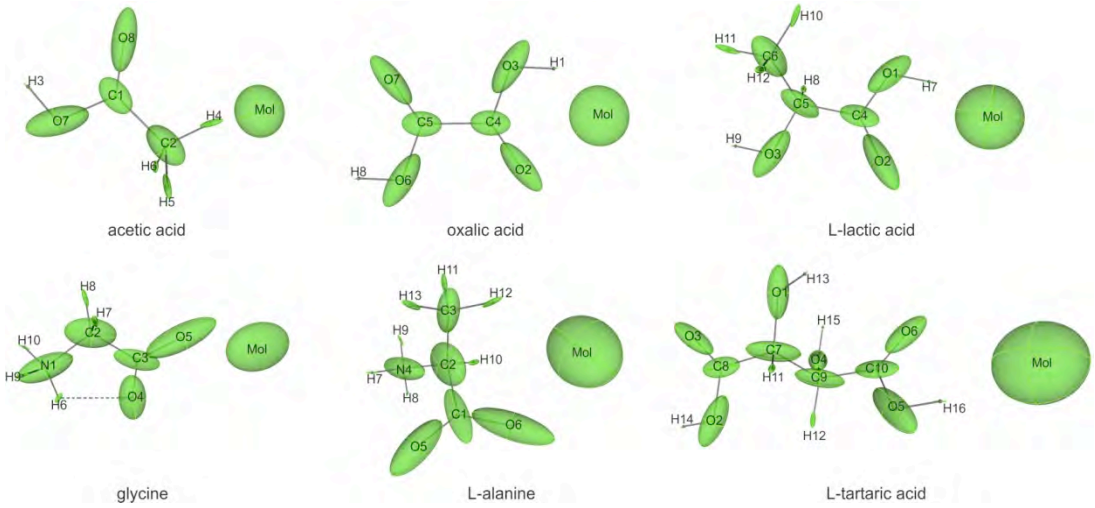

Figure 1 Graphical representation of distributed atomic and molecular (Mol) polarizabilities for some test molecules. The scaling factor for the atomic polarizabilities is 0.4 Å^{-2} (*i.e.* 1 Å^3 ≡ 0.4 Å) whereas for the molecular polarizability is 0.1 Å^{-2}.

Table 2 Bond parameters in a series of test molecules. d is the bond length of Ω-Ω', $d_Ω$ the distance between Ω and the bond critical point (bcp); $d_{Ω'}$ the distance between Ω' and bcp; $\rho(\mathbf{r_b})$ the electron density at bcp; $\nabla^2\rho(\mathbf{r_b})$ the Laplacian of electron density at bcp; ε the bond ellipticity; Q(Ω|Ω') the absolute value of the bond charge, $\alpha_{\parallel(\Omega)}$ and $\alpha_{\parallel(\Omega')}$ the polarizability components along the bond and α(Ω-Ω') the total bond polarizability. All quantities are in atomic units. For each kind of bond, averages and related standard deviations from the mean are calculated (excluding those bonds perturbed by intramolecular hydrogen bonding, as marked in red). X-H bonds are omitted from this table.

Bond (Ω-Ω')	**Molecule**	d	dΩ	dΩ'	$\rho(\mathbf{r_b})$	$\nabla^2\rho(\mathbf{r_b})$	**ε**	Q(Ω|Ω')	α||(Ω)	α||(Ω')	α(Ω-Ω')
C–C	Propanoic acid	2.88	1.47	1.41	0.24	-0.51	0.01	0.06	8.36	8.51	16.87
	L-lactic acid	2.90	1.42	1.48	0.24	-0.51	0.04	0.06	9.11	8.24	17.36
	Succinic acid	2.88	1.44	1.44	0.24	-0.53	0.02	0.00	8.80	8.80	17.60
	Glutaric acid	2.88	1.47	1.42	0.24	-0.52	0.02	0.06	9.37	8.92	18.29
	Glutaric acid	2.88	1.42	1.47	0.24	-0.52	0.02	0.06	8.92	9.38	18.30
	L-malic acid	2.90	1.46	1.44	0.24	-0.51	0.04	0.02	8.71	9.46	18.16
	L-tartaric acid	2.94	1.46	1.47	0.24	-0.47	0.05	0.00	9.14	9.26	18.41
	L-Glutamine	2.87	1.44	1.42	0.24	-0.53	0.02	0.02	8.99	8.71	17.70
	L-glutamic acid	2.89	1.42	1.48	0.24	-0.49	0.02	0.06	9.30	9.31	18.61
	L-valine	2.89	1.41	1.49	0.23	-0.48	0.01	0.03	7.47	7.67	15.14
Average		**2.89**	**1.44**	**1.45**	**0.24**	**-0.51**	**0.03**	**0.04**	**8.97**	**8.95**	**17.92**
Stand. Dev.		*0.02*	*0.02*	*0.03*	*0.00*	*0.02*	*0.01*	*0.03*	*0.30*	*0.40*	*0.54*
								0.06			
C–C(OOH)	Acetic acid	2.84	1.35	1.49	0.26	-0.61	0.06	0.14	8.75	7.59	16.34
	Propanoic acid	2.85	1.50	1.35	0.26	-0.60	0.08	0.16	7.93	8.72	16.65
	L-lactic acid	2.88	1.48	1.39	0.26	-0.60	0.11	0.11	8.03	7.97	16.00
	Oxalic acid	2.91	1.46	1.46	0.25	-0.56	0.11	0.00	7.54	7.54	15.08
	Malonic acid	2.86	1.48	1.38	0.25	-0.57	0.07	0.08	7.88	9.12	17.00
	Malonic acid	2.86	1.38	1.47	0.26	-0.60	0.05	0.08	8.59	7.53	16.12
	Succinic acid	2.85	1.49	1.36	0.26	-0.60	0.08	0.14	8.39	9.07	17.46
	Succinic acid	2.85	1.49	1.36	0.26	-0.60	0.08	0.14	8.39	9.07	17.46
	Glutaric acid	2.85	1.49	1.36	0.26	-0.60	0.08	0.14	8.56	9.54	18.10
	Glutaric acid	2.85	1.36	1.49	0.26	-0.60	0.08	0.14	9.53	8.56	18.09
	L-malic acid	2.87	1.49	1.38	0.26	-0.60	0.11	0.12	8.89	9.39	18.28
	L-malic acid	2.86	1.37	1.49	0.25	-0.59	0.07	0.11	9.69	8.64	18.33
	L-tartaric acid	2.88	1.41	1.47	0.25	-0.58	0.11	0.07	9.14	8.58	17.73
	L-tartaric acid	2.89	1.50	1.39	0.25	-0.58	0.10	0.13	8.82	9.09	17.91
	L-asparagine	2.87	1.47	1.40	0.25	-0.57	0.07	0.04	7.88	8.43	16.31
	L-glutamine	2.85	1.46	1.39	0.26	-0.59	0.07	0.06	9.01	10.37	19.38
	L-aspartic acid	2.86	1.35	1.51	0.25	-0.58	0.07	0.15	9.27	8.70	17.97
	L-glutamic acid	2.85	1.36	1.49	0.26	-0.60	0.07	0.13	8.29	7.80	16.09
Average		**2.86**	**1.44**	**1.43**	**0.26**	**-0.59**	**0.08**	**0.11**	**8.56**	**8.55**	**17.11**
Stand. Dev.		*0.02*	*0.06*	*0.06*	*0.01*	*0.01*	*0.02*	*0.04*	*0.60*	*0.63*	*0.96*
C–C(N)	L-alanine	2.88	1.40	1.48	0.24	-0.52	0.03	0.08	9.16	8.73	17.89
	L-asparagine	2.87	1.46	1.41	0.24	-0.53	0.03	0.05	9.60	9.41	19.02
	L-glutamine	2.88	1.40	1.49	0.24	-0.52	0.02	0.10	10.30	10.38	20.68
	L-aspartic acid	2.89	1.48	1.42	0.24	-0.49	0.02	0.04	9.07	9.13	18.20
	L-glutamic acid	2.90	1.41	1.49	0.24	-0.50	0.03	0.08	8.64	8.77	17.41
	L-valine	2.88	1.38	1.49	0.24	-0.52	0.04	0.06	7.89	8.05	15.95
Average		**2.88**	**1.43**	**1.46**	**0.24**	**-0.51**	**0.03**	**0.07**	**9.35**	**9.28**	**18.64**
Stand. Dev.		*0.01*	*0.03*	*0.04*	*0.00*	*0.02*	*0.01*	*0.02*	*0.56*	*0.60*	*1.15*
(N)C–C(OOH)	Glycine	2.84	1.36	1.49	0.26	-0.61	0.08	0.57	11.16	10.33	21.49
	L-alanine	2.90	1.38	1.52	0.24	-0.54	0.08	0.73	12.45	10.92	23.36
	L-asparagine	2.91	1.37	1.54	0.24	-0.51	0.08	0.71	10.71	9.37	20.07
	L-glutamine	2.90	1.52	1.38	0.24	-0.53	0.08	0.73	9.89	11.41	21.30
	L-aspartic acid	2.91	1.37	1.53	0.24	-0.53	0.07	0.73	11.90	10.05	21.94
	L-glutamic acid	2.90	1.38	1.52	0.25	-0.54	0.07	0.75	11.85	9.65	21.51
	L-valine	2.92	1.39	1.52	0.24	-0.51	0.08	0.70	10.67	8.83	19.49
Average		**2.91**	**1.40**	**1.50**	**0.24**	**-0.53**	**0.08**	**0.73**	**11.25**	**10.04**	**21.28**
Stand. Dev.		*0.03*	*0.06*	*0.06*	*0.01*	*0.03*	*0.00*	*0.06*	*0.89*	*0.89*	*1.26*
C–N	Glycine	2.78	1.04	1.73	0.24	-0.61	0.04	0.20	8.71	11.93	20.64
	L-alanine	2.81	1.06	1.75	0.23	-0.54	0.04	0.36	9.82	13.11	22.93
	L-asparagine	2.51	0.94	1.57	0.34	-1.15	0.14	0.32	7.02	13.80	20.82
	L-asparagine	2.83	1.07	1.76	0.23	-0.51	0.06	0.37	8.26	10.79	19.04
	L-glutamine	2.52	0.95	1.57	0.34	-1.14	0.14	0.32	6.97	14.27	21.24
	L-glutamine	2.83	1.07	1.76	0.23	-0.51	0.04	0.36	9.22	12.40	21.62
	L-aspartic acid	2.81	1.05	1.77	0.23	-0.51	0.05	0.37	7.73	10.02	17.75
	L-glutamic acid	2.83	1.05	1.78	0.22	-0.49	0.03	0.37	7.79	10.38	18.18
	L-Valine	2.82	1.05	1.77	0.23	-0.51	0.02	0.37	8.47	11.07	19.55

Average		**2.75**	**1.03**	**1.72**	**0.26**	**-0.67**	**0.07**	**0.36**	**8.16**	**11.98**	**20.14**
Stand. Dev.		*0.13*	*0.05*	*0.08*	*0.05*	*0.28*	*0.05*	*0.06*	*0.95*	*1.53*	*1.69*
C–O	Formic acid	2.54	0.89	1.65	0.31	-0.74	0.02	0.50	5.06	11.20	16.26
	Acetic acid	2.57	0.91	1.66	0.30	-0.77	0.02	0.50	4.91	11.52	16.42
	Propanoic acid	2.57	0.91	1.66	0.30	-0.76	0.02	0.51	5.06	12.05	17.12
	L-lactic acid	2.57	0.91	1.66	0.30	-0.76	0.02	0.50	4.79	11.43	16.22
	L-lactic acid	2.67	0.99	1.69	0.27	-0.70	0.04	0.49	4.30	11.51	15.81
	Oxalic acid	2.53	0.89	1.64	0.32	-0.79	0.05	0.47	4.95	11.09	16.04
	Oxalic acid	2.53	0.89	1.64	0.32	-0.79	0.05	0.47	4.95	11.09	16.04
	Malonic acid	2.56	0.91	1.65	0.31	-0.78	0.03	0.49	5.34	12.07	17.41
	Malonic acid	2.55	0.90	1.65	0.31	-0.77	0.04	0.49	4.77	11.26	16.03
	Succinic acid	2.56	0.91	1.66	0.30	-0.77	0.02	0.50	5.42	12.09	17.51
	Succinic acid	2.56	0.91	1.66	0.30	-0.77	0.02	0.50	5.42	12.09	17.50
	Glutaric acid	2.57	0.91	1.66	0.30	-0.76	0.02	0.50	5.44	12.39	17.84
	Glutaric acid	2.57	0.91	1.66	0.30	-0.76	0.02	0.50	5.44	12.39	17.84
	L-malic acid	2.54	0.89	1.65	0.31	-0.75	0.02	0.50	5.10	11.19	16.29
	L-malic acid	2.66	0.99	1.68	0.27	-0.73	0.05	0.49	4.33	11.34	15.67
	L-malic acid	2.56	0.90	1.65	0.31	-0.77	0.03	0.50	5.50	12.24	17.74
	L-tartaric acid	2.56	0.91	1.66	0.30	-0.76	0.03	0.50	4.63	11.05	15.68
	L-tartaric acid	2.56	0.90	1.66	0.30	-0.75	0.02	0.50	5.11	11.59	16.71
	L-tartaric acid	2.67	0.98	1.69	0.27	-0.70	0.03	0.48	3.94	10.53	14.47
	L-tartaric acid	2.64	0.97	1.67	0.28	-0.74	0.01	0.48	4.18	10.91	15.09
	L-aspartic acid	2.49	0.85	1.63	0.33	-0.64	0.02	0.54	4.72	10.60	15.32
	L-glutamic acid	2.49	0.86	1.63	0.33	-0.67	0.03	0.53	5.35	11.67	17.02
Average		**2.57**	**0.91**	**1.66**	**0.30**	**-0.75**	**0.03**	**0.50**	**4.94**	**11.51**	**16.46**
Stand. Dev.		*0.05*	*0.04*	*0.02*	*0.02*	*0.04*	*0.01*	*0.02*	*0.44*	*0.54*	*0.92*
COO-	Glycine	2.30	0.79	1.51	0.42	-0.57	0.10	1.05	5.21	12.40	17.60
	Glycine	2.51	0.96	1.55	0.34	-1.01	0.13	1.04	8.13	17.72	25.85
	L-alanine	2.36	0.82	1.54	0.39	-0.77	0.11	1.20	5.55	13.79	19.34
	L-alanine	2.39	0.85	1.54	0.38	-0.91	0.13	1.14	6.97	15.76	22.72
	L-asparagine	2.34	0.82	1.53	0.40	-0.74	0.11	1.21	5.33	13.61	18.94
	L-asparagine	2.37	0.84	1.54	0.39	-0.87	0.12	1.17	5.85	14.35	20.20
	L-glutamine	2.34	0.81	1.53	0.40	-0.71	0.11	1.22	5.13	12.99	18.12
	L-glutamine	2.38	0.84	1.54	0.38	-0.88	0.13	1.15	6.38	14.93	21.31
	L-aspartic acid	2.38	0.84	1.54	0.38	-0.83	0.12	1.19	5.47	13.91	19.38
	L-aspartic acid	2.37	0.84	1.54	0.39	-0.85	0.14	1.15	6.89	15.36	22.25
	L-glutamic acid	2.36	0.83	1.53	0.39	-0.83	0.13	1.16	6.95	15.19	22.14
	L-glutamic acid	2.39	0.84	1.55	0.38	-0.86	0.12	1.19	5.39	14.24	19.64
	L-valine	2.39	0.84	1.55	0.38	-0.84	0.11	1.20	5.37	14.28	19.65
	L-valine	2.36	0.83	1.53	0.39	-0.83	0.13	1.11	6.28	13.93	20.21
Average		**2.36**	**0.83**	**1.54**	**0.39**	**-0.81**	**0.12**	**1.16**	**5.91**	**14.21**	**20.12**
Stand. Dev.		*0.02*	*0.01*	*0.01*	*0.01*	*0.06*	*0.01*	*0.03*	*0.70*	*0.81*	*1.46*
C=O	Formic acid	2.26	0.78	1.48	0.44	-0.53	0.12	1.13	5.26	11.06	16.32
	Acetic acid	2.27	0.79	1.49	0.43	-0.59	0.13	1.15	6.01	11.68	17.69
	Propanoic acid	2.28	0.79	1.49	0.43	-0.58	0.12	1.15	5.72	11.21	16.92
	L-lactic acid	2.26	0.78	1.48	0.44	-0.53	0.12	1.13	5.86	11.49	17.35
	Oxalic acid	2.26	0.78	1.48	0.44	-0.53	0.13	1.10	5.82	11.38	17.20
	Oxalic acid	2.26	0.78	1.48	0.44	-0.53	0.13	1.10	5.82	11.38	17.20
	Malonic acid	2.27	0.79	1.48	0.43	-0.57	0.14	1.14	5.82	11.69	17.51
	Malonic acid	2.27	0.79	1.48	0.44	-0.57	0.13	1.13	5.40	10.85	16.24
	Succinic acid	2.28	0.79	1.49	0.43	-0.59	0.12	1.15	5.36	11.08	16.44
	Succinic acid	2.28	0.79	1.49	0.43	-0.59	0.12	1.15	5.36	11.08	16.44
	Glutaric acid	2.27	0.79	1.49	0.43	-0.58	0.12	1.15	5.49	10.97	16.46
	Glutaric acid	2.27	0.79	1.49	0.43	-0.58	0.12	1.15	5.49	10.97	16.46
	L-malic acid	2.27	0.79	1.49	0.43	-0.58	0.12	1.14	5.40	11.05	16.45
	L-malic acid	2.28	0.79	1.49	0.43	-0.58	0.11	1.14	5.78	11.60	17.38
	L-tartaric acid	2.26	0.78	1.48	0.44	-0.51	0.13	1.12	6.19	11.79	17.98
	L-tartaric acid	2.27	0.78	1.48	0.43	-0.54	0.12	1.14	5.75	11.44	17.18
	L-asparagine	2.34	0.82	1.52	0.40	-0.82	0.11	1.11	4.86	10.80	15.66
	L-glutamine	2.32	0.81	1.51	0.41	-0.76	0.11	1.13	5.62	12.34	17.96
	L-aspartic acid	2.31	0.80	1.50	0.42	-0.72	0.13	1.12	6.20	12.45	18.65
	L-glutamic acid	2.31	0.81	1.50	0.42	-0.72	0.13	1.12	4.91	10.39	15.30
Average		**2.28**	**0.79**	**1.49**	**0.43**	**-0.60**	**0.12**	**1.13**	**5.61**	**11.34**	**16.94**
Stand. Dev.		*0.02*	*0.01*	*0.01*	*0.01*	*0.08*	*0.01*	*0.02*	*0.36*	*0.49*	*0.80*

As discussed above one of our purposes is the visualization of atomic polarizability tensors, which are extremely informative to understand the formation of a molecular property. In Figure 1, we see atomic and molecular polarizabilities for some mono- and di- carboxylic acids and some amino acids in their zwitterionic configuration. It is interesting in general to note the pronounced elongation of the atomic ellipsoids in the direction of the more polarizable bonds. This is for example quite typical for the O atoms of carbonylic, as well as in oxydrilic groups, in keeping with the idea that these bonds are highly polarizable, because containing a softer π bonding and a large electronegativity difference. In carbonylic groups, the Oxygen polarizability tensor is symmetrical (or quasi-symmetrical) respect to the C=O bond axis, unless it is involved in a hydrogen bonding (see for example the intramolecular bond in neutral configuration of glycine in Figure 1). In oxydrilic oxygens, the tensor is not symmetrical respect to the C-O bond, because of the O-H bond which slightly rotates the Oxygen polarizability tensor. The carbon atom is normally less prolate in the direction of C=O or C-O bonds, because attached to other atoms (H, C or N in the molecules we investigated). Interestingly, all atoms have smaller polarizability components in the direction of a X-H bond, whereas the H atoms have a highly prolate shape (but of course the hydrogen polarizability tensor is in general very small, due to the small electronic population of the H atom).

The analysis of Figure 1 and Table 2 also shows that functional groups have very similar (atomic or group) polarizabilities in different molecules and this speaks for a good exportability of these quantities, as it is already known for the atomic electronic moments (???). However, intermolecular interactions can substantially modify the atomic polarizability, for example hydrogen bonding. In O-H…O bonds, there are two very visible effects: a) the hydrogen atom becomes more polarizable, beside

normally it is more positively charged; b) the HB acceptor modifies the shape and orientation of its polarizability tensor, which is stretched in the direction of the HB.

As we mentioned above, the presence of a ring makes the calculation of atomic polarizabilities more arbitrary, because depending on the additional constraint necessary for the ring. It is very interesting to compare what happens in glycine, for both the neutral and zwitterionic configurations that we calculated. In Figure 2, we show the distributed polarizabilites calculated using equation (8) (same scheme as proposed by Keith), equation (9) with bond weights as defined in (10) or excluding the hydrogen bond from the calculation. All three schemes perfectly reconstruct the total molecular polarizability, of course, but it seems that the weighted scheme better represents the expected continuity between a scenario with or without a weak hydrogen bond. Noteworthy, the main changes affect the hydrogen bond acceptor atom. The "popular" scheme (*i.e.* "one bond, one vote") instead drastically changes the atomic polarizabilities, even when the hydrogen bond is very weak. For this reason, this scheme, although equally exact, is less informative.

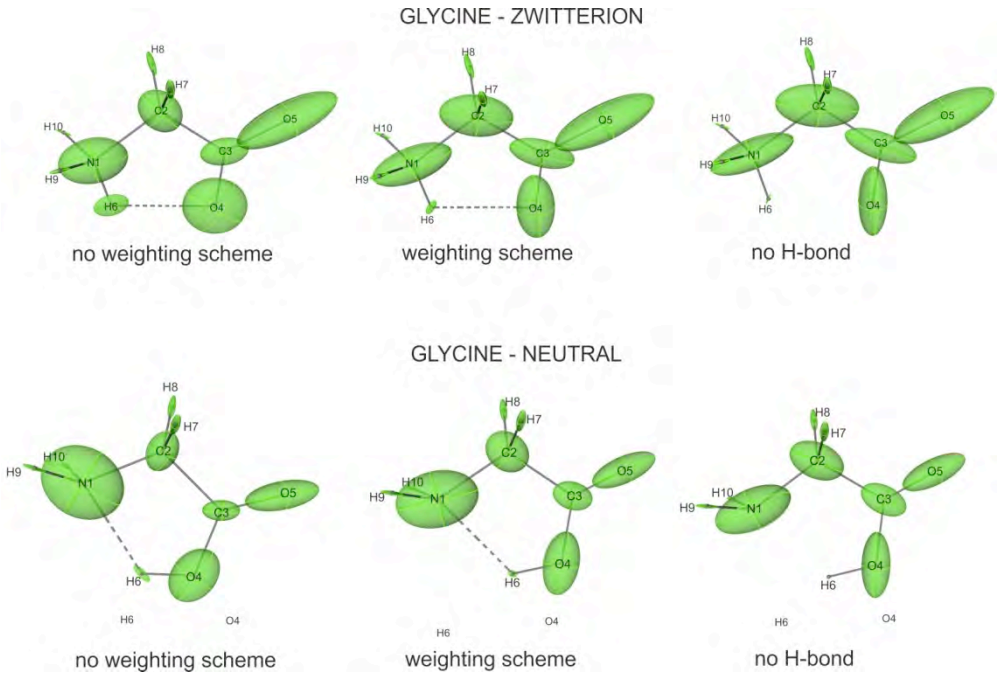

Figure 2 Graphical representation of the distributed atomic polarizabilities in glycine for both the neutral and zwitterionic configurations. For each configuration the different treatments of the ring produced by the weak intramolecular N-H...O bond is shown: a) on the left, all bonds in the ring are treated for some test molecules; b) in the central picture, a weighted scheme is adopted with weights inversely proportional to the electron density at the critical point; c) on the right, the intramolecular hydrogen bond is not counted at all. Scale factors as in Figure 1.

It is very interesting also to observe what happens in aromatic rings. In Figure 3, there are three examples. In the simple benzene molecule, the atomic ellipsoids nicely show the preferred polarization in the ring. In this molecule, of course the scheme (8) and (9) are identical, because of the symmetry. In substituted benzene, like p-nitro-aniline, instead, the perturbation produce by the nitro and amino groups are very visible and the ellipsoids are definitely more elongated along the NO_2----NH_2 axis. In acenaphthenequinonediimine (BIAN), a common ligand used in metal catalysis, we see the distributed polarizabilities in polycyclic systems.

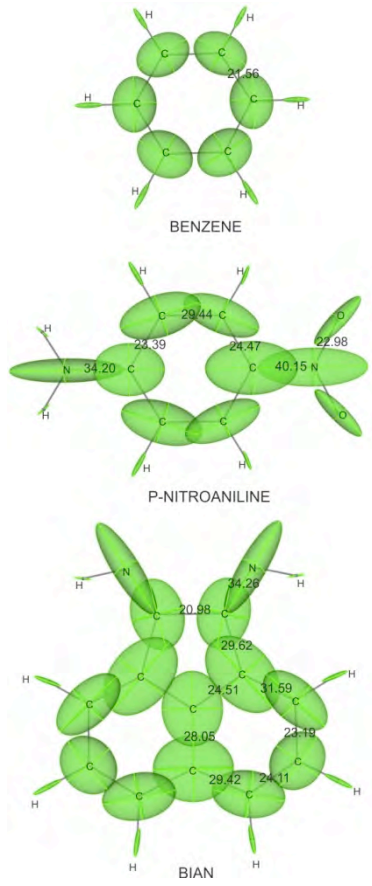

Figure 3 Graphical representation of the distributed atomic polarizabilities in benzene, p-nitro-aniline (PAN) and in acenaphthenequinonediimine (BIAN). Scale factors as in Figure 1. Bond polarizabilities are indicated (in a.u.) for all bonds, but the X-H ones.

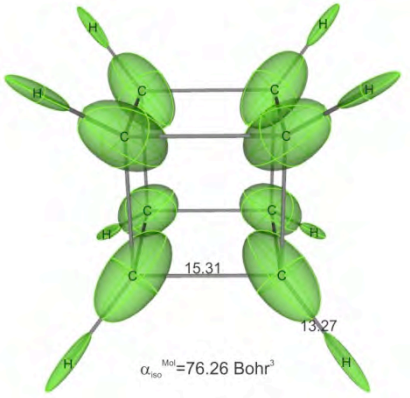

Figure 4 Graphical representation of the distributed atomic polarizabilities in cubane. Scale factors as in Figure 1. Bond polarizabilities are indicated (in a.u.) for all bonds, isotropic molecular polarizability is also given.

In Figure 4, we see also the distributed polarizabilities in cubane, i.e. a molecule where each C atom is involved in three cycles forming overall a cage. Applying equation (11) with extension for all ring conditions, the bond induced charges come straightforwardly and therefore the atomic polarizabilities are easily computed.

Noteworthy, the three fold site symmetry produce carbon ellipsoids prolated in C-H direction.

The calculations we carried out offer also the opportunity to evaluate the *bond polarizability* α_{bond}, a quantity that is usually advocated in the literature but very often it is not really defined. Here we have instead an easy and quantitative definition, coming from the projection of $\boldsymbol{\alpha}_{\Omega}$ and $\boldsymbol{\alpha}_{\Omega'}$ tensors along the **Ω-Ω'** bond:

$$\alpha_{\Omega-\Omega'} = \mathbf{r}_{\Omega\Omega'}^{T} \cdot (\boldsymbol{\alpha}_{\Omega} + \boldsymbol{\alpha}_{\Omega'}) \cdot \mathbf{r}_{\Omega\Omega'} \qquad (16)$$

where $\mathbf{r}_{\Omega\Omega'}$ is a unit vector in the direction **Ω-Ω'**.

The bond polarizability is therefore a scalar showing how feasible is the polarization of the electron density along the bond, upon application of an electric field in the same direction.

Bond polarizabilities (which are also measured in $Bohr^3$) are reported in the pictures of Figure 3 for the aromatic rings there discussed and quantitatively represent the visual impression produced by the ellipsoids elongation.

It is also interesting to investigate the distributed atomic polarizabilities of transition metal complexes. We report here just one example, which is quite illustrative, $Cr(CO)_6$, see Figure 5. The compound is quite proto-typical of organometallic complexes. It is particularly interesting to compare the CO ligand, which is a closed shell stable molecule, in isolation or coordinated to the metal. In CO, the O atom is highly polarized along the C-O bond, whereas the C atom is much less. Overall the bond polarizability is not large (15.4 $Bohr^3$), in keeping with the high bond order. In the coordinated compound, however, the C atom changes completely the polarizability tensor, which is now highly prolated in Cr-C direction. This causes a much higher C-O polarizability (34.1 $Bohr^3$), in keeping with the typical bond elongation and weakening due to metal to ligand π back-donation process.

Noteworthy is anyway the very large atomic polarizability of Cr atom, which is of course spherical because of the octahedral site symmetry.

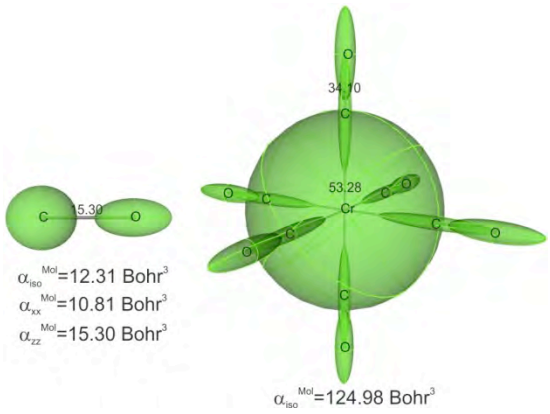

Figure 5 Graphical representation of the distributed atomic polarizabilities in isolated CO and in $Cr(CO)_6$. Bond polarizabilities are indicated (in a.u.). Scale factors as in Figure 1. The total isotropic molecular polarizability is also indicated. For CO, the total isotropic as well as the parallel (ZZ) and perpendicular (XX) components are indicated.

The calculations we have reported here allow to investigate what other atomic quantities are correlated with the atomic polarizabilities. It is intuitive that an electron distribution is more polarizable the larger is the total number of electrons and the larger is the volume used by the electrons. Consequently, the isotropic polarizability

$$\alpha_{iso}(\Omega) = \frac{1}{3}(\alpha_{XX}(\Omega) + \alpha_{YY}(\Omega) + \alpha_{ZZ}(\Omega)) \qquad (17)$$

is somewhat related with the product $N(\Omega)V(\Omega)$, where $N(\Omega)$ is the atomic population and $V(\Omega)$ the atomic volume. This is visible in Figures 6a-6c, where scatterplots for O, C and H atoms are shown. For O and H atoms the correlation is more obvious, whereas for C atoms is less visible (although it becomes more evident if we group entries by functional groups, see Figure 6b).

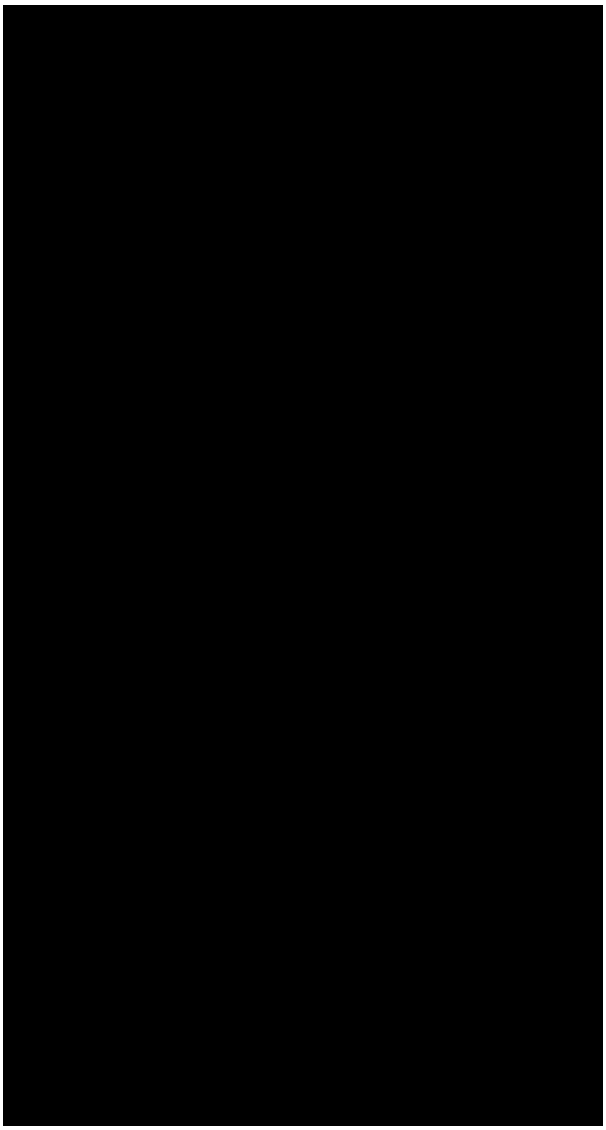

Figure 6 Scatterplots of isotropic atomic polarizabilities against atomic electrons x volume for Oxygen, Carbon and Hydrogen atoms calculated in the molecules reported in Table 2.

The second obvious evidence is that atomic polarizability tensors are stretched in direction of the chemical bonds, so they are directly related to the electron polarization induced by the chemical bonding. This could be visible by comparing the distributed atomic polarizabilities in a simple molecule, like urea, and the electron density distribution (better emphasized by the deformation density, see Figure 7).

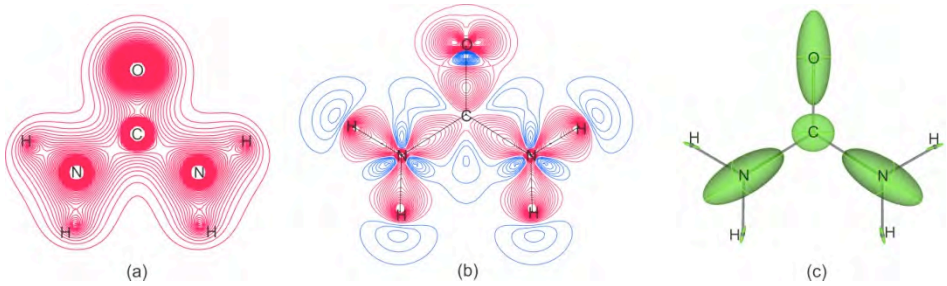

Figure 7. Total electron density (a), deformation density (b) and atomic polarizabilities (c) in urea.

This correlation can certainly be used to estimate the atomic polarizability from the electron density distribution, as we will extensively investigate in future work. Some empirical relations between polarizabilities and electron density distribution have been proposed (Fkyerat, *et al.* (1995); Fkyerat, *et al.* (1996); Hamzaouia, Zanouna & Vergoten (2004)), based on molecular electric moments. This approach received criticism by Whitten, Jayatilaka and Spackman (2006), who instead proposed two more reliable approximations, based only on the occupied molecular orbitals, calculated through an X-ray constrained wave function approach. Although simple and accurate, this model still requires a molecular orbital approach, therefore it cannot be straightforwardly applied to an electron density distribution (as for example available from experiments, through multipolar expansion, see Hansen and Coppens (1978)). Contrary to proposals by Fkyerat, *et al.* (1995); Fkyerat, *et al.* (1996); Hamzaouia, Zanouna & Vergoten (2004), it seems clear that an empirical correlation between electron distribution and polarizability is better constructed after partitioning in terms of atomic polarizabilities and if the atomic charges, volumes and anisotropies are properly taken into account. We expect to develop a simple electron density based model in the next future.

Another application of the distributed atomic polarizabilities is the calculation of intensities of Raman scattering, by derivation of $\boldsymbol{\alpha}$ along a normal mode. In particular,

if the mode coincide with a given bond, then it is easy to numerically differentiate the bond polarizability $\alpha_{A\text{-}B}$ (to give $\alpha'_{\parallel}$) and therefore compute the Raman intensities and the atomic contributions to that. For example, in CO there is only one mode (bond stretching). The bond polarizability derivative ($\alpha'_{\parallel}$ = 9.3 Bohr^2) is directly proportional to the Raman intensity, but C and O have different contribution to (3.2 and 6.1 Bohr^2, respectively), that could be used to analyze the individual atomic contribution to a given Raman intensity. Noteworthy, also the polarizability change perpendicular to the bond is relevant, and can be of course calculated ($\alpha'_{\perp}$ = 1.06 Bohr^2; $\alpha'_{\perp}$(C) = 0.31 Bohr^2; $\alpha'_{\perp}$(O) = 0.75 Bohr^2), again confirming that O has the larger contribution.

Conclusions

In this paper, we have investigated QTAIM distributed atomic polarizabilities with the intent to extract more chemical information from a quantity that can be calculated with precision at quantum chemical level, but that is normally not analysed in details.

In particular, we have proposed a different and more reliable way to partition the polarizability in case of "loops" in the molecular graph. We have also proposed a way to visualize the atomic polarizabilities, which is extremely informative to show which factors mostly affect these quantities. Moreover, we have introduced an indicator for the bond polarizability, obtained as the sum of projected atomic polarizability over a bond.

The applications of this approach are enormous and we summarize here the plan for the near future.

Larger molecules, organometallic polymers and crystals. It appears from this study that distributed atomic polarizabilities are quite transferable, when functional groups

are properly defined. This allows calculating semi-empirical molecular polarizabilities for larger molecules at low costs. Corrections due to intermolecular bonding can be easily incorporated. This could be particularly for the calculation of crystal optic properties, like for example refractive indexes, using atomic polarizabilities for each functional group of the molecular species.

Modelling from experimental electron density. The tight relationship between atomic polarizabilities and atomic electron density can be further exploited trying to improve the current empirical models that tentatively reconstruct a molecular polarizability from multipolar expanded electron density distributions. This could facilitate the estimation of the polarizability tensors directly from experiment.

Intermolecular energies. A better quality distributed atomic polarizabilities could be useful for the evaluation of induction energies (interaction between external electric field and molecular polarizability) and dispersion energies (mutual interaction between polarizabilities) in simulations of macromolecules as well as crystal packed species.

Hyper-polarizabilities. An extension of the current approach could provide the distributed atomic hyper-polarizabilities, based on double (or higher) derivatives of the dipolar density of eq. (4) with respect to the field. This would open access to evaluation of non linear optic properties in crystal, as well.

Acknowledgements

We thank Swiss CRUS for financial support (sciex NMS boursary 10.083). Prof. D. Jayatilaka is thanked for several useful discussions and comments.

References

Bader, R.F.W. (1989) J. Chem. Phys. **91**, 6989-7001.

Bader, R.F.W. (1990) *Atoms in Molecules: A Quantum Theory,* Oxford University Press, Oxford, UK, **1990**.

Bader, R.F.W., Keith, T.A., Gough, K.M. & Laidig K.E. *Mol. Phys.* (1992) **75**, 1167-1189.

Bader, R.F.W., Larouche, A., Gatti, C., Carroll, M.T., MacDougall, P.J. & Wiberg, K.B. (1987) *J.Chem.Phys.* **87**, 1142-1152.

Dittrich, B., Koritsanszky, T. & Luger, P. (2004) *Angew. Chem. Int. Ed. Engl.* **43**, 2718–2721.

Dittrich, B., Hübschle, C.B., Luger, P. & Spackman, M.A. (2006) *Acta Cryst. D* **62**, 1325–1335.

Domagała, S. & Jelsch, C. (2008) *J. Appl. Cryst.* **41**, 1140–1149.

Dominiak, P.M., Volkov, A., Li, X., Messerschmidt, M. & Coppens, P. (2007) *J. Chem. Theory Comput.* **3***,* 232-247.

Fkyerat, A., Guelzim, A., Baert, F., Paulus, W., Heger, G., Zyss, J. & Périgaud, A. (1995) *Acta Cryst.*, **B51**, 197-209.

Fkyerat, A., Guelzim, A., Baert, F., Zyss, J. & Périgaud, A. (1996) *Phys. Rev. B*, **53**, 16236-16246.

Hamzaoui, F., Zanoun, A. & Vergoten, G. (2004) *Journal of Molecular Structure* **697**, 17–22.

Hansen, N. K. & Coppens P. (1978) *Acta Cryst*, **A34**, 909-921

Kamburelis, M. (2011) view3dscene(version 3.10.1), http://castle-engine.sourceforge.net.

Keith, T.A. (2007) *Atomic Response Properties* in *The Quantum Theory of Atoms in Molecules: From Solid State to DNA and Drug Design* Matta C.F., Boyd R.J., Eds., Wiley-VCH, Weinheim, **2007**.

Keith, T.A. (2011) AIMAll, Version 11.10.16**,** aim.tkgristmill.com.

Nye, J.F (1985) *Physical Properties of Crystals: Their Representation by Tensors and Matrices*, Oxford University Press.

Laidig K.E. & Bader. R.F.W. (1990) *J. Chem. Phys.* **93**, 7213-7224.

Le Sueur, C.R. & Stone, A.J. (1993) *Molecular Physics*, **78**, 1267-1291.

Pichon-Pesme, V., Jelsch, C., Guillot, B. & Lecomte, C. (2004) *Acta Cryst. A* **60**, 204-208.

Pichon-Pesme, V., Lecomte, C. & Lachekar, H. (1995) *J. Phys. Chem.,* **99**, 6242–6250.

Stone, A. J. (1985) *Molecular Physics*, **56**, 1065-1082.

Volkov, A., Li, X., Koritsanszky, T. & Coppens, P. (2004) *J. Phys. Chem. A* **108**, 4283-4300.

Whitten, A.E., Jayatilaka, D. & Spackman, M.A. (2006) *J. Chem. Phys.*, **125**, 174505-174515.

Zarychta, B., Pichon-Pesme, V., Guillot, B., Lecomte C. & Jelsch C. (2007) *Acta Cryst.* **A63**, 108-125.